LETTER

The evolution of cooperation within the gut microbiota

Seth Rakoff-Nahoum[1,2], Kevin R. Foster[3] & Laurie E. Comstock[2]

Cooperative phenotypes are considered central to the functioning of microbial communities in many contexts, including communication via quorum sensing, biofilm formation, antibiotic resistance, and pathogenesis[1–5]. The human intestine houses a dense and diverse microbial community critical to health[1,2,4–9], yet we know little about cooperation within this important ecosystem. Here we test experimentally for evolved cooperation within the Bacteroidales, the dominant Gram-negative bacteria of the human intestine. We show that during growth on certain dietary polysaccharides, the model member *Bacteroides thetaiotaomicron* exhibits only limited cooperation. Although this organism digests these polysaccharides extracellularly, mutants lacking this ability are outcompeted. In contrast, we discovered a dedicated cross-feeding enzyme system in the prominent gut symbiont *Bacteroides ovatus*, which digests polysaccharide at a cost to itself but at a benefit to another species. Using *in vitro* systems and gnotobiotic mouse colonization models, we find that extracellular digestion of inulin increases the fitness of *B. ovatus* owing to reciprocal benefits when it feeds other gut species such as *Bacteroides vulgatus*. This is a rare example of naturally-evolved cooperation between microbial species. Our study reveals both the complexity and importance of cooperative phenotypes within the mammalian intestinal microbiota.

A major challenge facing the study of host-associated microbiotas is to understand the ecological and evolutionary dynamics that shape these communities[2,5,10–13]. A key determinant of microbial dynamics is the balance of cooperation and competition both within and between species[2,5,14,15]. Here we test for the evolution of cooperation within the mammalian microbiota by focusing on the Bacteroidales, the most abundant order of Gram-negative bacteria of the human intestine with species that co-colonize the host at high densities of 10^9–10^{11} CFU per gram of faeces[16,17]. Members of this order break down polysaccharides outside of their cell using outer surface glycoside hydrolases[6,18], some of which are secreted on outer membrane vesicles[3,19]. This suggests a significant potential for one cell to cooperatively feed other cells. As extracellular digestion is considered important for growth of Bacteroidales on polysaccharides[1,6,8], we focused on this trait as a candidate for cooperative interactions within the gut microbiota and asked whether a bacterium that breaks down a polysaccharide extracellularly receives most, or all[20], of the benefits of its efforts.

We first made isogenic mutants in genes responsible for the extracellular digestion of polysaccharides in the well-studied human gut strain, *Bacteroides thetaiotaomicron* VPI-5482 (refs 1, 8). Specifically, we deleted the genes encoding the outer surface glycoside hydrolases BT3698 of the amylopectin/starch utilization locus and BT1760 of the levan utilization locus (Fig. 1a), required for growth on amylopectin and levan, respectively (Fig. 1b, c, Extended Data Fig. 1a, b). Consistent with previous observations[1,8], neither mutant grew with the specific polysaccharide in monoculture (Fig. 1b, c, Extended Data Fig. 1a, b). However, co-culture of ΔBT3698 or ΔBT1760 with wild type in amylopectin or levan

increased the fitness of the mutants (Fig. 1d, e, Extended Data Fig. 1c, d). This is consistent with cooperation via public good availability of amylopectin and levan breakdown products.
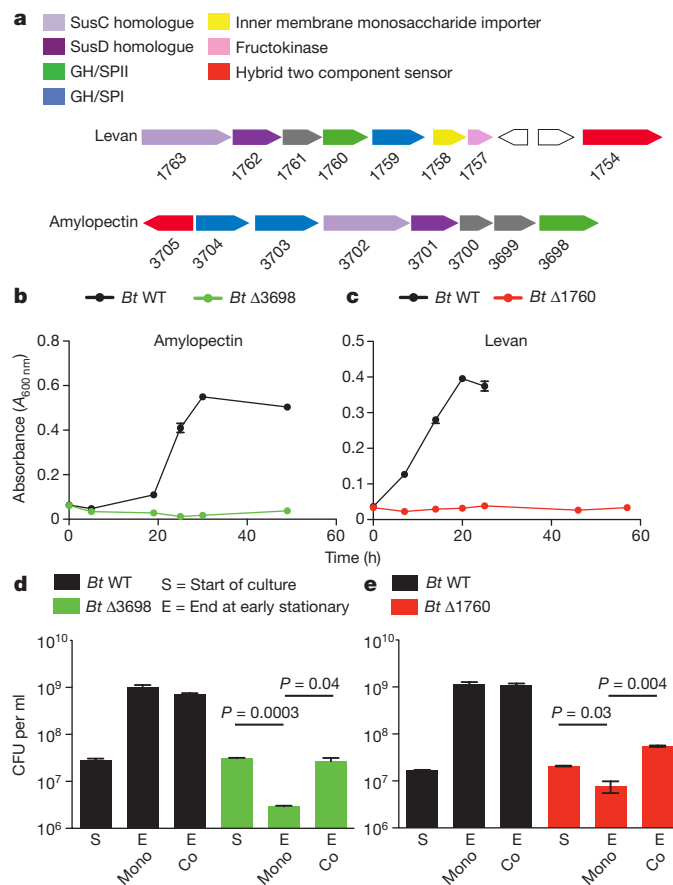

Figure 1 | Direct and cooperative benefits of polysaccharide digestion by surface glycoside hydrolases (GH). a, Polysaccharide utilization loci of *B. thetaiotaomicron* (*Bt*) for amylopectin and levan with the products or properties each gene encodes listed above and colour-coded. SPI or SPII, signal peptidase I or II cleavage site, respectively. **b**, **c**, Growth of *Bt* wild type (WT) and surface GH mutants in media with amylopectin ($n = 2$, cell culture biological replicates) (**b**) or levan ($n = 2$, cell culture biological replicates) (**c**). See Extended Data Fig. 1 for additional independent experiments. **d**, **e**, Growth of *Bt* WT and surface GH mutants in mono- and co-culture in media with amylopectin ($n = 2$, cell culture biological replicates) (**d**) or levan ($n = 2$, cell culture biological replicates) (**e**). See Extended Data Fig. 1 for additional independent experiments. In all panels error bars represent standard error; *P* values derived from two-tailed Student's *t*-test.

[1]Division of Infectious Diseases, Department of Medicine, Boston Children's Hospital and Harvard Medical School, 300 Longwood Avenue, Boston, Massachusetts 02115, USA. [2]Division of Infectious Diseases, Department of Medicine, Brigham and Women's Hospital and Harvard Medical School, 181 Longwood Avenue, Boston, Massachusetts 02115, USA. [3]Department of Zoology and Oxford Centre for Integrative Systems Biology, University of Oxford, Oxford OX1 3PS, UK.
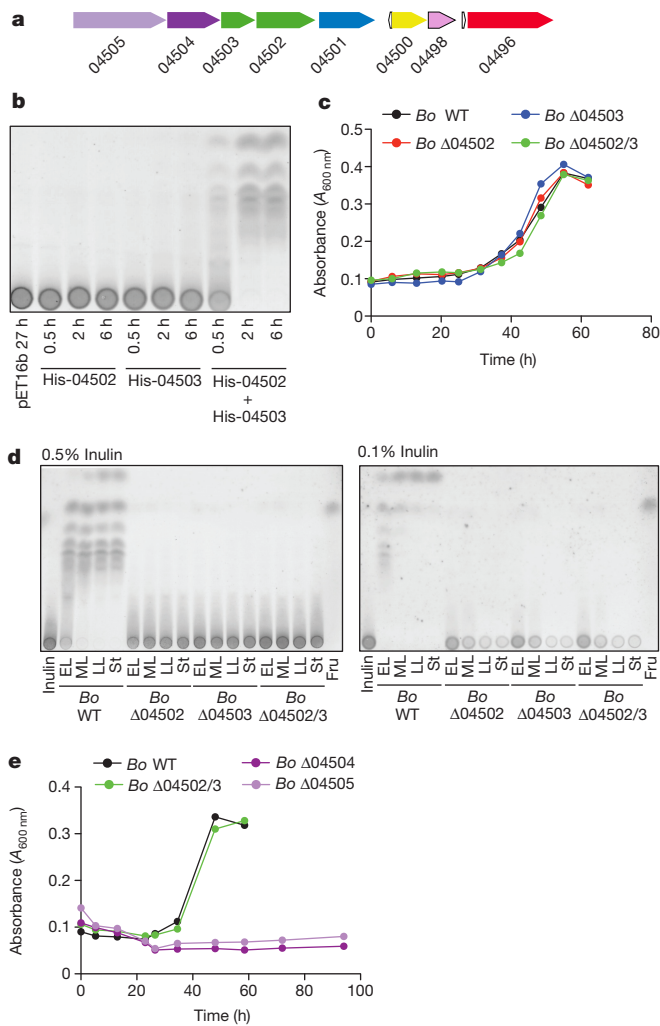
Figure 2 | *B. ovatus* does not require surface digestion for utilization of inulin. a, Predicted inulin utilization locus of *B. ovatus* (*Bo*). Gene designations shown are preceded by BACOVA_. The colour coding of gene products is as in Fig. 1. **b**, Thin layer chromatography (TLC) analysis of inulin defined medium incubated for the indicated times with purified His-tagged 04502, 04503 or 04502 and 04503, or vector control. See Supplementary Information Fig. 1 for uncropped scanned images. **c**, Growth of *Bo* WT and mutants in inulin defined medium. **d**, TLC analysis of conditioned media during the growth of *Bo* WT and mutants in 0.5% and 0.1% inulin. EL, early log; ML, mid log; LL, late log; St, stationary. **e**, Growth of *Bo* WT, Δ04502/3, Δ04504 (*susD* orthologue) and Δ04505 (*susC* orthologue) mutants in inulin defined medium. For **c**, **e**, each line represents $n = 1$ sample per condition. See Extended Data Fig. 2 for additional independent experiments. In all panels error bars represent standard error; *P* values derived from two-tailed Student's *t*-test.

One of the key questions in evolutionary biology is how cooperative systems can be evolutionarily stable[4,5,14,21,22]. If certain cells invest in the production of an enzyme that helps others, what prevents these cells from being outcompeted by cells that consume the breakdown products without making the enzyme? In the *B. thetaiotaomicron* amylopectin and levan polysaccharide utilization systems, while receiving public goods from the wild type benefits the mutant cells (Fig. 1d, e, Extended Data Fig. 1e), they do not outcompete the wild type. Cells that make the enzyme receive more benefits than non-producing neighbouring cells. This observation suggests that a cell can utilize the majority of the polysaccharide that it breaks down, and that these private[23] benefits are central to the evolutionary stability of extracellular polysaccharide digestions in these systems.
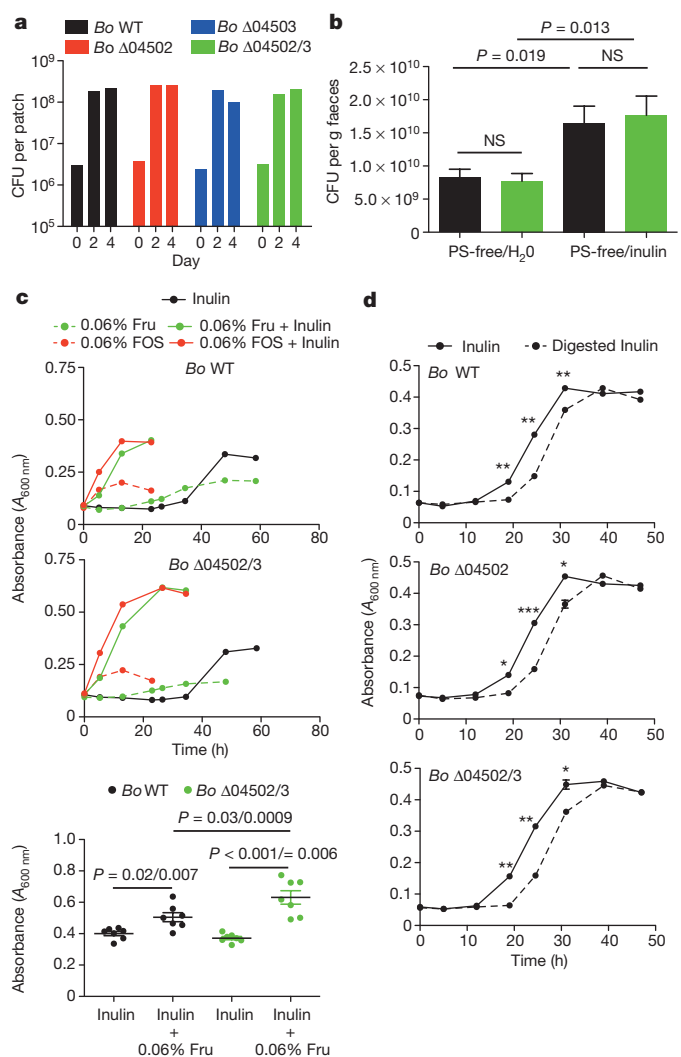
Figure 3 | Cost of inulin digestion by surface glycoside hydrolases. a, Growth yield of *Bo* WT and mutants on inulin agarose plates. Each line represents $n = 1$ sample per condition. See Extended Data Fig. 4 for additional independent experiments. **b**, Bacteria per gram of faeces of gnotobiotic mice seven days after monocolonization with *Bo* WT or Δ04502/3 on a polysaccharide-free diet or supplemented with inulin ($n = 5$ biological replicate mice per condition). **c**, Growth curves (upper and middle panels) and maximal $A_{600\,nm}$ (bottom panel) of *Bo* WT or Δ04502/3 in minimal media with carbon sources as indicated. Each line represents $n = 1$ sample per condition. See Extended Data Fig. 4 for additional independent experiments. In the bottom panel, *P* values are displayed as paired (matched WT and Δ04502/3 within same experiment) followed by unpaired (all experiments) two-tailed Student's *t*-test ($n = 7$, biological replicates). **d**, Growth of *Bo* WT or mutants in inulin or a stoichiometric equivalent amount of inulin breakdown products after digestion with purified 04502 and 04503 enzymes ($n = 2$, cell culture biological replicates); *$P < 0.05$; **$P < 0.01$; ***$P < 0.001$; see Extended Data Fig. 5 for additional independent experiments. In all panels error bars represent standard error; *P* values derived from two-tailed Student's *t*-test.

We extended our analysis to another prominent member of the human Bacteroidales known to extensively utilize polysaccharides, *Bacteroides ovatus* (*Bo*)[24]. During growth on inulin, a dietary fructan known for health-promoting effects[25], *Bo* extracellularly digests and liberates considerable amounts of inulin breakdown products[3]. The predicted inulin utilization locus of the *Bo* type strain ATCC 8483 encodes two similar outer surface glycoside hydrolases, BACOVA_04502 and BACOVA_04503 (Fig. 2a), both of which are predicted to target the β1,2 inulin fructose polymer[1,3]. Both of these enzymes are required for
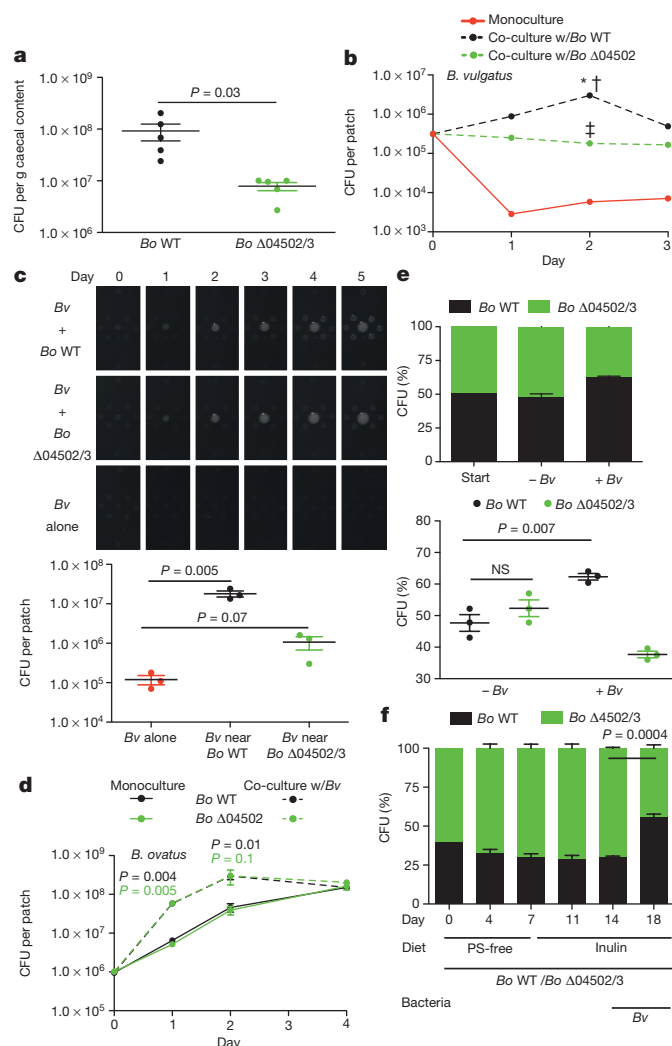
Figure 4 | Interspecies cooperation mediated by surface digestion of inulin is stabilized by reciprocal benefits. a, Germ-free mice were monocolonized with *Bo* WT or Δ04502/3 and maintained on a polysaccharide-free diet supplemented with inulin and housed for 2 weeks. Mice were then gavaged with the caecal contents of conventionally raised mice. At day 5 post gavage, caecal contents were plated for enumeration of *Bo* (*n* = 5 biological replicate mice per group). **b**, Enumeration of *Bv* in monoculture or co-culture with *Bo* WT or Δ04502 on defined inulin plates. *P = 0.001 for number of *Bv* in *Bv*/*Bo* WT co-culture vs *Bv* alone; †*P* = 0.001 for number of *Bv* in *Bv*/*Bo* WT co-culture vs *Bv*/Δ04502 co-culture; ‡*P* = 0.003 for number of *Bv* in *Bv*/Δ04502 co-culture vs *Bv* alone (*n* = 2, cell culture biological replicates). See Extended Data Figs 7 and 9 for additional independent experiments. **c**, (left) Photos of patches of *Bv* plated at varying distances around *Bo* WT or *Bo* Δ04502/3 or alone on inulin agarose plates. (right) Enumeration of *Bv* after five days of culture plated at the same distance to *Bo* WT or *Bo* Δ04502/3 or alone on inulin plates. See Extended Data Fig. 9 for additional independent experiments. **d**, Enumeration of *Bo* WT or Δ04502 in monoculture or co-culture with *Bv* on defined inulin plates. *P* values correlate to colour of line/genotype used for statistical analysis. *P* value indicates comparison of monoculture and co-culture for the given condition at the time-point indicated. The benefit *Bo* receives from *Bv* is most robust when starting with fewer *Bo*. Depicted are starting CFU of ~10^6 *Bo*. (*n* = 3, cell culture biological replicates at day 1, 2; *n* = 2, biological replicates at day 4). See Extended Data Fig. 7 for additional independent experiments and Extended Data Fig. 7b for starting CFU of ~10^7 *Bo*. **e**, Ratios of wild type and Δ04502/3 at the start and day 2 of culture when co-plated with or without *Bv* on inulin plates (*n* = 3, cell culture biological replicates). See Extended Data Fig. 9 for additional independent experiments. **f**, Ratios of WT and Δ04502/3 in the inoculum (day 0) and in faeces at various time points (days 4, 7, 11, 14, 18) post co-colonization of gnotobiotic mice (*n* = 3 cell culture biological replicates) with *Bo* WT and Δ04502/3. Polysaccharide-free diet was supplemented with inulin at day 7. *Bv* was introduced at day 14. A Fisher exact test comparing the frequency of *Bo* WT and Δ04502/3 pre- (day 14) and post- (day 18) colonization with *Bv* was significant with a *P* value of 0.0001 for each individual mouse. *Bo* CFU in faeces were maximal after the switch to inulin diet and addition of *Bv* changed the abundance of *Bo* WT compared to Δ04502/3 but not total CFU of *Bo*. See Extended Data Fig. 9 for additional independent experiments. In all panels error bars represent standard error; *P* values displayed are derived from two-tailed Student's *t*-test.

inulin breakdown (Fig. 2b). We therefore predicted that a single mutant of either BACOVA_04502 or BACOVA_04503 would be unable to grow on inulin. Surprisingly, neither of the single deletion mutants (Δ04502 or Δ04503) nor the double mutant (Δ04502/3) demonstrated impaired fitness with inulin as the sole carbohydrate source (Fig. 2c, Extended Data Fig. 2a), even at limiting concentrations (Extended Data Fig. 2a).

Given the importance of extracellular polysaccharide digestion for growth of *Bacteroides* on numerous polysaccharides[1,6,8] (Fig. 1, Extended Data Fig. 1), we predicted that *Bo* synthesizes other enzymes that breakdown inulin extracellularly, allowing the *Bo* mutants to grow on this polysaccharide. However, analysis of the growth media of Δ04502, Δ04503 and Δ04502/3 revealed no released inulin breakdown products, demonstrating that BACOVA_04502 and BACOVA_04503 are solely responsible for extracellular digestion of inulin (Fig. 2d, Extended Data Fig. 2b; see Extended Data Fig. 2c for complementation). BACOVA_04504 and BACOVA_04505 encode SusD and SusC orthologues respectively, which are predicted to function in inulin binding and the import of digestion products[6,26]. Deletion of BACOVA_04504 or BACOVA_04505 resulted in significant impairment of growth on inulin (Fig. 2e, Extended Data Fig. 3a; see Extended Data Fig. 3b for complementation). Growth of Δ04502, Δ04503 and Δ04502/3 in limiting concentrations of inulin revealed depletion of inulin (Fig. 2d, right panel; Extended Data Fig. 2b). Together, these data demonstrate that surface enzymes 04502 and 04503 are not needed for *Bo* to utilize inulin, and suggest that inulin is directly imported via 04504–04505 without prior extracellular digestion.

Why would *Bo* synthesize surface/secreted enzymes that potently digest inulin outside of the cell if not necessary for its growth on the polysaccharide? A key evolutionary explanation for the release of secreted products by microbes is that they feed clonemates in a manner that is beneficial at the level of the clonal group[2,5,11,14,15]. We hypothesized that the importance of extracellular digestion may be realized during spatially structured growth on plates where not all cells are in direct contact with the polysaccharide. However, mutant bacteria showed no significant differences in growth yield compared to wild type on defined inulin plates (Fig. 3a; Extended Data Fig. 4a). In addition, these enzymes were not required for optimal growth *in vivo* as wild type and Δ04502/3 showed equal colonization levels in gnotobiotic mice fed a polysaccharide-free diet with inulin added as the sole dietary polysaccharide (Fig. 3b). Therefore, we could find no evidence that inulin breakdown by 04502 and 04503 benefits *Bo* in three-dimensional growth or during monocolonization of the mammalian gut.

Bacteroidales polysaccharide utilization loci can be induced by monomers or oligomers of the cognate polysaccharide[1,26]. This raised the possibility that 04502 and 04503 may be important for optimal growth on inulin during induction. However, although addition of trace amounts of fructose monomers or oligosaccharides led to accelerated growth on inulin (Fig. 3c, Extended Data Fig. 4b), this did not require 04502/3 (Fig. 3c, Extended Data Fig. 4b). Rather than a benefit from the presence of the enzymes, we observed a cost based on reduced yield of the wild type compared to Δ04502/3 mutant during induced growth (Fig. 3c, Extended Data Fig. 4b) that was independent of a direct energetic cost of synthesis of 04502/3 (Figs 2c, e, 3c, d and Extended Data Figs 2a, 4b and 5a, b, c). We find that *Bo* grows better on undigested inulin than an equal concentration of inulin breakdown products (Fig. 3d, Extended Data Fig. 5a, b). In addition, the yield advantage to the

mutant does not occur under limiting inulin concentrations (Extended Data Fig. 5d,e). Furthermore, *Bo* preferentially consumes longer inulin digestion products over shorter oligomers and fructose (Fig. 2d, right panel, Extended Data Fig. 2b, right panel). Together, these data suggest that undigested inulin is the preferred substrate of *Bo*, and that extracellular digestion by 04502/3 under certain conditions is costly for fitness.

We found no evidence that extracellular digestion of inulin by *Bo* evolved for cooperation with clonemates. Therefore, we speculated that this trait might have evolved for cooperation with other species in the gut. We first sought evidence of cooperation in the setting of a natural gut ecosystem. Germ-free mice were fed inulin and colonized with either *Bo* wild type or Δ04502/3 followed by the introduction of the caecal microbiota of conventionally raised mice. *Bo* wild type and Δ04502/3 equally colonized mice before the introduction of the microbiota (Extended Data Fig. 6a), but *Bo* wild type received a significant fitness benefit compared to Δ04502/3 in the context of a complex microbiota (Fig. 4a). These data suggested that, although not required for *Bo* to utilize inulin, 04502 and 04503 provide a benefit to *Bo* only realized in a community setting. The conditions for the evolution of cooperation between species are much more restrictive than those within a clone. In particular, theory predicts that costly interspecies cooperation will only be stabilized if there are reciprocal feedback benefits, such as a plant providing nectar for an insect that pollinates it[21,22]. From this experiment, we identified two dominant mouse microbiota Bacteroidales strains that thrived on *Bo*-derived inulin breakdown products (Extended Data Fig. 6b), with delayed growth on inulin (Extended Data Fig. 6b). These data suggest that cross-feeding Bacteroidales members may provide reciprocal benefits to wild-type *Bo* in the mammalian gut.

To test experimentally for reciprocity and benefits of inulin digestion between species, we used an inulin co-culture system with *Bo* wild type or Δ04502 and *Bacteroides vulgatus* ATCC 8482 (*Bv*), which is commonly found together with *Bo* at high densities in humans[16,17] and thrives on inulin breakdown products[3] but cannot use inulin[1,3]. Co-culture and proximate plating with *Bo* wild type increased the fitness of *Bv* compared to that with Δ04502 (Fig. 4b, c and Extended Data Figs 7a, 9a); however, *Bv* is able to persist better with Δ04502 than when alone (Fig. 4b, Extended Data Fig. 7a), owing to a small (<2,000 Da) secreted molecule(s) that contributes to the survival of *Bv* (Extended Data Fig. 8a, b). This 04502/3-independent survival is not mediated by a universal factor made by *Bacteroides* during growth on inulin nor *Bo*-derived short-chain fatty acids (Extended Data Fig. 8a, c, d). Thus, there are multiple mechanisms by which *Bo* helps *Bv* (Fig. 4b, Extended Data Fig. 7a), the greatest being cross-feeding mediated by 04502/3.

We next addressed the question of whether *Bo* receives reciprocal benefits from *Bv*. Co-culture of *Bv* with *Bo* on plates increased the fitness of *Bo* wild type and *Bo* Δ04502 (Fig. 4d, Extended Data Fig. 7b), but did not increase the fitness of *B. fragilis* (Extended Data Fig. 7c). If inulin breakdown can be costly, and *Bo* receives benefits from *Bv* irrespective of whether inulin is broken down and fed to *Bv*, natural selection is expected to favour the loss of the genes encoding the secreted inulin glycoside hydrolases[22]. However, our pairwise experiments would not reveal the possibility that *Bo* wild type receives more reciprocal benefits from *Bv* when in direct competition with the non-cross-feeding mutant[21,27]. Therefore, we co- and tri-cultured these strains on plates and compared the yields of the two *Bo* strains (wild type and Δ04502/3) with or without *Bv*. Addition of *Bv* leads to an increased proportion of *Bo* wild type compared to the Δ04502/3 mutant (Fig. 4e, Extended Data Fig. 9b). We extended these studies to a gnotobiotic mouse colonization model. *Bo* wild type had no advantage in direct competition with Δ04502/3 on a polysaccharide-free diet or when inulin is added (Fig. 4f). However, introduction of *Bv* increased the fitness of the *Bo* wild type relative to the mutant (Fig. 4f, Extended Data Fig. 9c, d). Together, these data suggest that extracellular breakdown of inulin

increases the fitness of *Bo* via reciprocal benefits from another species. These findings are consistent with the evolution of cooperation between species within the gut microbiota.

We find evidence of distinct forms of cooperativity within the Bacteroidales of the human intestinal microbiota (Extended Data Fig. 10). For *B. thetaiotaomicron*, amylopectin and levan digestion provide mostly private benefits and modest social benefits to other cells. By contrast, *Bo* releases large amounts of inulin digestion products via a pair of dedicated cross-feeding secreted enzymes unnecessary for its use of inulin. These enzymes allow for cooperation with cross-fed species, which provide benefits in return. Potential mechanisms by which *Bv* may provide return benefits to *Bo* include detoxification of inhibitory substances, or production of a depleted or growth promoting factor, the latter supported by early growth benefits to *Bo* via *Bv* secreted factors (Extended Data Fig. 9e).

Understanding whether microbial communities are formally cooperative is central to predicting their evolutionary and ecological stability. Cooperative systems can be productive, but are prone to instabilities on both ecological and evolutionary timescales that can undermine them[5,14,15,21,22]. The ability of one species to utilize the waste product of another is prevalent, but waste production alone does not signify cooperative evolution. As opposed to waste product utilization or exploitive interactions[28–30], there are few well-documented cases of evolved cooperation between microbial species where one species evolves to help another[14]. We have found evidence of strong eco-evolutionary interactions within the microbiota that are likely to be central to the functioning of these complex communities.

1. Sonnenburg, E. D. *et al.* Specificity of polysaccharide use in intestinal bacteroides species determines diet-induced microbiota alterations. *Cell* **141**, 1241–1252 (2010).
2. West, S. A., Griffin, A. S., Gardner, A. & Diggle, S. P. Social evolution theory for microorganisms. *Nature Rev. Microbiol.* **4**, 597–607 (2006).
3. Rakoff-Nahoum, S., Coyne, M. J. & Comstock, L. E. An ecological network of polysaccharide utilization among human intestinal symbionts. *Curr. Biol.* **24**, 40–49 (2014).
4. Drescher, K., Nadell, C. D., Stone, H. A., Wingreen, N. S. & Bassler, B. L. Solutions to the public goods dilemma in bacterial biofilms. *Curr. Biol.* **24**, 50–55 (2014).
5. Frank, S. A. A general model of the public goods dilemma. *J. Evol. Biol.* **23**, 1245–1250 (2010).
6. Koropatkin, N. M., Cameron, E. A. & Martens, E. C. How glycan metabolism shapes the human gut microbiota. *Nature Rev. Microbiol.* **10**, 323–335 (2012).
7. Subramanian, S. *et al.* Cultivating healthy growth and nutrition through the gut microbiota. *Cell* **161**, 36–48 (2015).
8. Shipman, J. A., Cho, K. H., Siegel, H. A. & Salyers, A. A. Physiological characterization of SusG, an outer membrane protein essential for starch utilization by Bacteroides thetaiotaomicron. *J. Bacteriol.* **181**, 7206–7211 (1999).
9. Littman, D. R. & Pamer, E. G. Role of the commensal microbiota in normal and pathogenic host immune responses. *Cell Host Microbe* **10**, 311–323 (2011).
10. Waldor, M. K. *et al.* Where next for microbiome research? *PLoS Biol.* **13**, e1002050 (2015).
11. Koschwanez, J. H., Foster, K. R. & Murray, A. W. Sucrose utilization in budding yeast as a model for the origin of undifferentiated multicellularity. *PLoS Biol.* **9**, e1001122 (2011).
12. Costello, E. K., Stagaman, K., Dethlefsen, L., Bohannan, B. J. M. & Relman, D. A. The application of ecological theory toward an understanding of the human microbiome. *Science* **336**, 1255–1262 (2012).
13. Estrela, S., Whiteley, M. & Brown, S. P. The demographic determinants of human microbiome health. *Trends Microbiol.* **23**, 134–141 (2015).
14. Mitri, S. & Foster, K. R. The genotypic view of social interactions in microbial communities. *Annu. Rev. Genet.* **47**, 247–273 (2013).
15. Oliveira, N. M., Niehus, R. & Foster, K. R. Evolutionary limits to cooperation in microbial communities. *Proc. Natl Acad. Sci. USA* **111**, 17941–17946 (2014).
16. Faith, J. J. *et al.* The long-term stability of the human gut microbiota. *Science* **341**, 1237439 (2013).

17. Zitomersky, N. L., Coyne, M. J. & Comstock, L. E. Longitudinal analysis of the prevalence, maintenance, and IgA response to species of the order Bacteroidales in the human gut. *Infect. Immun.* **79,** 2012–2020 (2011).
18. Flint, H. J., Bayer, E. A., Rincon, M. T., Lamed, R. & White, B. A. Polysaccharide utilization by gut bacteria: potential for new insights from genomic analysis. *Nature Rev. Microbiol.* **6,** 121–131 (2008).
19. Elhenawy, W., Debelyy, M. O. & Feldman, M. F. Preferential packing of acidic glycosidases and proteases into Bacteroides outer membrane vesicles. *mBio* **5,** e00909–14 (2014).
20. Cuskin, F. *et al.* Human gut Bacteroidetes can utilize yeast mannan through a selfish mechanism. *Nature* **517,** 165–169 (2015).
21. Sachs, J. L., Mueller, U. G., Wilcox, T. P. & Bull, J. J. The evolution of cooperation. *Q. Rev. Biol.* **79,** 135–160 (2004).
22. Foster, K. R. & Wenseleers, T. A general model for the evolution of mutualisms. *J. Evol. Biol.* **19,** 1283–1293 (2006).
23. Gore, J., Youk, H. & van Oudenaarden, A. Snowdrift game dynamics and facultative cheating in yeast. *Nature* **459,** 253–256 (2009).
24. Martens, E. C. *et al.* Recognition and degradation of plant cell wall polysaccharides by two human gut symbionts. *PLoS Biol.* **9,** e1001221 (2011).
25. Orel, R. & Kamhi Trop, T. Intestinal microbiota, probiotics and prebiotics in inflammatory bowel disease. *World J. Gastroenterol.* **20,** 11505–11524 (2014).
26. Cameron, E. A. *et al.* Multifunctional nutrient-binding proteins adapt human symbiotic bacteria for glycan competition in the gut by separately promoting enhanced sensing and catalysis. *mBio* **5,** e01441–14 (2014).
27. Momeni, B., Waite, A. J. & Shou, W. Spatial self-organization favors heterotypic cooperation over cheating. *Elife* **2,** e00960 (2013).
28. Ng, K. M. *et al.* Microbiota-liberated host sugars facilitiate post-antobiotic expansion of enteric pathogens. *Nature* **502,** 96–99 (2013).
29. Degnan, P. H., Barry, N. A., Mok, K. C., Taga, M. E. & Goodman, A. L. Human gut microbes use multiple transporters to distinguish vitamin B$_{12}$ analogs and compete in the gut. *Cell Host Microbe* **15,** 47–57 (2014).
30. Fischbach, M. A. & Sonnenburg, J. L. Eating for two: how metabolism establishes interspecies interactions in the gut. *Cell Host Microbe* **10,** 336–347 (2011).

Author Contributions S.R.-N. performed mutant construction bacterial cultures, gnotobiotic experiments, protein purification and TLC, L.E.C. assisted with mutant construction. S.R.-N. and L.E.C. analysed the data. S.R.-N., K.R.F. and L.E.C. designed the study and wrote the paper.

Author Information Reprints and permissions information is available at www.nature.com/reprints. The authors declare no competing financial interests. Readers are welcome to comment on the online version of the paper. Correspondence and requests for materials should be addressed to S.R.-N. (seth.rakoff-nahoum@childrens.harvard.edu).

METHODS

Bacterial strains and media. Bacteroidales type strains used in this study are *Bo* ATCC 8483, *B. thetaiotaomicron* VPI 5482 *Bv* ATCC 8482, and *B. fragilis* NCTC 9343. Bacteria were grown in media formulation as previously described[3].

Bacterial culture. For growth in defined media, bacteria were inoculated from brain heart infusion plates containing haemin and vitamin K (BHIS) plates into basal medium (BS), cultured overnight to stationary phase, then diluted 1:10 in fresh BS and grown to mid log. At mid log, bacteria were pelleted by centrifugation and washed with sterile phosphate buffered saline (PBS) and then inoculated in defined media. Carbohydrates used to supplement defined media include fructose (F2543, Sigma), fructose oligosaccharides (FOS; OraftiP95, Beneo-Orafti group), levan (L8647, Sigma), amylopectin (10120, Sigma), and inulin (OraftiHP, Beneo-Orafti group). Levan and amylopectin were autoclaved as 1% w/v in H_2O and dialysed using 3.5 kDa MW membranes (Slide-A-Lyzer Dialysis Cassettes, ThermoScientific). Short chain fatty acids acetate, propionate and succinate were purchased from Sigma. Stock solutions of 2 mM were pH neutralized to pH 7.2–7.3 with 10 N NaOH. All cultures were grown at 37 °C under anaerobic conditions. Bacterial growth was quantified by absorbance ($A_{600\,nm}$) using 200 μl of bacterial culture in 96-well flat-bottom microtitre plates using a Powerwave spectrophotometer (Biotek). Murine gut Bacteroidales from the caecal preparations used in for the colonization experiments were grown on BHIS plates. Resulting colonies were tested for growth in inulin minimal medium or inulin breakdown products from the conditioned media of *Bo* grown in inulin, containing inulin breakdown products as previously described[3].

Creation of *Bacteroides* mutants. Deletion mutants were created whereby the genes encoding BT3698 or BT1760 in *Bacteroides thetaiotaomicron* VPI 5482, BACOVA_04502 in *Bo* ATCC 8483 BACOVA_04503, BACOVA_04502/3, BACOVA_04504, or BACOVA_04505 in *Bo* ATCC 8483 were removed. DNA segments upstream and downstream of the region to be deleted were PCR amplified using the primers outlined in Supplementary Table 1. PCR products were digested with BamHI, EcoRI and/or MluI engineered into the primers (Supplementary Information Table 1) and cloned by three-way ligation into the appropriate site of pNJR6 (ref. 31). The resulting plasmids were conjugally transferred into the *Bacteroides* strain as indicated using helper plasmid R751 and cointegrates were selected by erythromycin resistance. Cross outs were screened by PCR for the mutant genotype.

Cloning of PUL genes for expression in deletion mutants. BACOVA_04502, BACOVA_04503, BACOVA_04502/3, BACOVA_04504, BACOVA_04505 or BACOVA_04504/5 genes were PCR amplified using the primers listed in Supplementary Table 1. The PCR products were digested and ligated into the BamHI or KpnI site of the *Bacteroides* expression vector pFD340[32]. Plasmids containing the correct orientation of the insert in relation to the vector-borne promoter were introduced into mutant *Bacteroides* strains by mobilization from *E. coli* using helper plasmid RK231.

Mono-, co- and tri- culture experiments. For bacterial mono and co-culture experiments in defined liquid media, bacteria were grown as indicated for monoculture before addition to the defined media. Sterile magnetic stir bars were added to culture tubes within a rack placed on a stir plate within the anaerobic chamber. For conditioned media experiments, *Bo* WT, *Bo* Δ04502, *Bo* Δ04502/3, *Bv*, or *Bf* were grown to early log in inulin defined media or 0.125% fructose defined media (for Extended Data Fig. 9e), conditioned media were collected, filter sterilized, and incubated at 37 °C for 72 h. Conditioned media was replenished with defined media without additional carbohydrate and used for cultivation of *Bv*. *Bo* Δ04502/3 conditioned media was dialysed in defined media without carbohydrate using 2 kDa MW membranes (Slide-A-Lyzer Dialysis Cassettes, ThermoScientific). For monoculture of *Bo* WT and mutants on solid agarose, 4 μl of the indicated concentration of bacteria were dotted onto minimal inulin agarose plates. At the indicated time points, the bacteria were cut out, diluted and plated onto BHIS for CFU enumeration. For co-plating experiments, 10^6 *Bo* (WT or mutant) or *Bf* were co-plated with 10^5 *Bv* or a control volume of PBS. Four μl were then dotted on to defined inulin agarose plates. At the indicated time points, the dotted patches were cut from the agarose plates and resuspended in PBS, diluted and plated to BHIS for enumeration. Quantification and differentiation of wild type and isogenic glycoside hydrolase or polysaccharide lyase mutant was performed by plating dilutions of mixed liquid culture or the cut-out patch on agarose plates onto BHIS, followed by picking ∼100 colonies and determining wild type or mutant genotype by PCR using primers listed in Supplementary Table 1. For genotypic screening of *B. thetaiotaomicron* wild type and *B. thetaiotaomicron* Δ3698, two sets of primers were used (Supplementary Table 1). For *Bo*/*Bv* co-culture in Fig. 4b, c and Extended Data Fig. 7, *Bo* Δ03533 (WT) and *Bo* Δ03533 Δ04502 (Δ04502) arginine auxotrophic mutants were used in co-culture with *Bv* on minimal inulin agarose plates supplemented with 50 μg ml^{-1} of arginine (Sigma) which does not impair or limit

growth as compared to wild type[3]. Colonies on BHIS plates were replica plated onto defined glucose defined plates, which support the growth of *Bv* but not *Bo* Δ03533 or *Bo* Δ03533 Δ04502.

Thin-layer chromatography. Thin-layer chromatography (TLC) was employed to specifically detect carbohydrates as previously described[3]. Standards for TLC included glucose (G7528, Sigma), fructose (F2543, Sigma), fructose oligosaccharides (FOS; OraftiP95, Beneo-Orafti group) and inulin (OraftiHP, Beneo-Orafti group). See Supplementary Information Fig. 1 for uncropped TLCs.

Gas chromatographic analysis of culture media. Chromatographic analysis was carried out using a Shimadzu GC14-A system with a flame ionization detector (FID) (Shimadzu Corp, Kyoto, Japan). A volatile acid mix containing 10 mM of acetic, propionic, isobutyric, butyric, isovaleric, valeric, isocaproic, caproic, and heptanoic acids was used (Matreya, Pleasant Gap PA). A non-volatile acid mix containing 10 mM of pyruvic and lactic acid and 5 mM of oxaloacetic, oxalic, methyl malonic, malonic, fumaric, and succinic acid was used (Matreya, Pleasant Gap PA).

Cloning, purification, and enzymatic analysis of BACOVA_04502-3. To obtain purified BACOVA_04502 and BACOVA_04503 proteins, these genes were cloned individually into the BamHI site of pET16b (Novagen) using the primers listed in Supplementary Table 1. The constructs were designed so that the His-tag encoded by pET16b replaced the SpII signal sequence of these proteins allowing for their solubility. The recombinant plasmids were transformed into *E. coli* BL21 (DE3), grown to an $A_{600\,nm}$ of 0.6–0.7, and expression of the recombinant gene was induced by the addition of 0.4 mM IPTG for an additional 4 h. The His-tagged proteins were isolated essentially as described[33] using Dynabeads TALON paramagnetic beads. For enzymatic analysis (Fig. 2a) the proteins were added to inulin media in their magnetic bead-bound form. This allows for easy removal of the enzymes following digestion. As a control, the beads resulting from the same procedure performed with *E. coli* (DE3) containing only the vector (pET16b) were used. For *Bo* growth assays (Fig. 3d), 50 μl of beads (25 μl containing His-04502 and 25 μl containing His-04503) or equivalent volume of Dynabead buffer (for undigested inulin) were added to inulin defined medium. After 24 h at 37 °C, the beads containing the enzyme were removed with a magnet, and the media (digested or undigested inulin) was used to culture *Bo* WT and Δ04502.

Gnotobiotic mouse experiments. All animal experiments were approved by the Harvard Medical School IACUC. Swiss Webster germ-free male mice (6–10 weeks old) were purchased from the Harvard Digestive Diseases Gnotobiotic Core facility. Littermates were randomly allocated for different gnotobiotic experimental arms. Experiments were conducted in either sterile Optima cages (Figs 3b, 4a, Extended Data Fig. 9d) or gnotobiotic isolators (Fig. 4f). When appropriate, animals were numbered by sterile tail markers for longitudinal analysis and were not blinded. Number of animals used for experimentation was determined by precedence for gnotobiotic studies. Longitudinal analysis in the experiment of Fig. 4f of the ratios of wild type to mutant *Bo* under changing environmental conditions allowed for internally-controlled, within-individual comparisons. Mice were placed on polysaccharide-free special chow (65% w/v glucose, protein-free, supplemented with all essential amino acids except arginine; BioServe). Arginine at 50 μg ml^{-1} was supplemented in all drinking water. As indicated, mice were given 1% inulin (w/v) in sterile drinking water. Mice were inoculated with the indicated bacteria by applying ∼10^8 live bacteria (grown to mid log) onto mouse fur. Dilutions of faeces at various time points following inoculation were plated to BHIS plates and genotyped as above (Fig. 4f). Predetermined exclusion criteria for gnotobiotic experiments contamination as determined by either the presence of colonies with distinct morphology on anaerobic plates than *Bo* or *Bv* or colonies present at >10^2 CFU ml^{-1} (limit of detection) under aerobic conditions.

For gavage of *Bo* WT or Δ04502/3 monocolonized mice with the caecal content of conventionalized raised mice, two ∼8-week-old male Swiss Webster mice purchased from Taconic and housed in a specific pathogen-free facility were euthanized under sterile conditions. Intestine was excised and care was made to leave caecum intact. Within 2 min of excision, the caeca were transferred into an anaerobic chamber where the caecal contents were pooled and diluted with ∼10 ml of pre-reduced phosphate buffered solution supplemented with 0.1% cysteine. Contents were vigorously vortexed and immediately divided equally into two conical flasks (one for each group of mouse) to ensure equality of suspension between both conical flasks. Tightly sealed conical flasks were transferred to the mouse facility at which point 200 μl were gavaged to each mouse housed in sterile Optima cages. Caecal contents were plated to LKV (Remel) plates for enrichment of Bacteroides. Different colony morphologies were assigned species by 16S PCR as previously described[17]. For each group of mice, mice were housed in cages of 2 and 3 mice per cage. At time of killing, caecal contents were collected and plated to defined inulin plates by which *Bo* was enumerated based on distinct colony morphology of Bo on inulin agarose plates that was not present in conventionally raised caecal population.

Statistical analysis. The experiments were not randomized, and the investigators were not blinded to allocation during experiments and outcome assessment. No statistical methods were used to predetermine sample size. Replicate experiments are shown in Extended Data. All P values are derived from Student's t-test except as indicated in Fig. 4f and Extended Data Fig. 9c where Fisher's exact test was performed. Statistical significance of variance reported as indicated per experiment in figure legends. All centre values are mean. Error bars are standard error of the mean.

31. Stevens, A. M., Shoemaker, N. B. & Salyers, A. A. The region of a Bacteroides conjugal chromosomal tetracycline resistance element which is responsible for production of plasmidlike forms from unlinked chromosomal DNA might also be involved in transfer of the element. *J. Bacteriol.* **172,** 4271–4279 (1990).
32. Smith, C. J., Rogers, M. B. & McKee, M. L. Heterologous gene expression in Bacteroides fragilis. *Plasmid* **27,** 141–154 (1992).
33. Coyne, M. J., Fletcher, C. M., Reinap, B. & Comstock, L. E. UDP-glucuronic acid decarboxylases of *Bacteroides fragilis* and their prevalence in bacteria. *J. Bacteriol.* **193,** 5252–5259 (2011).
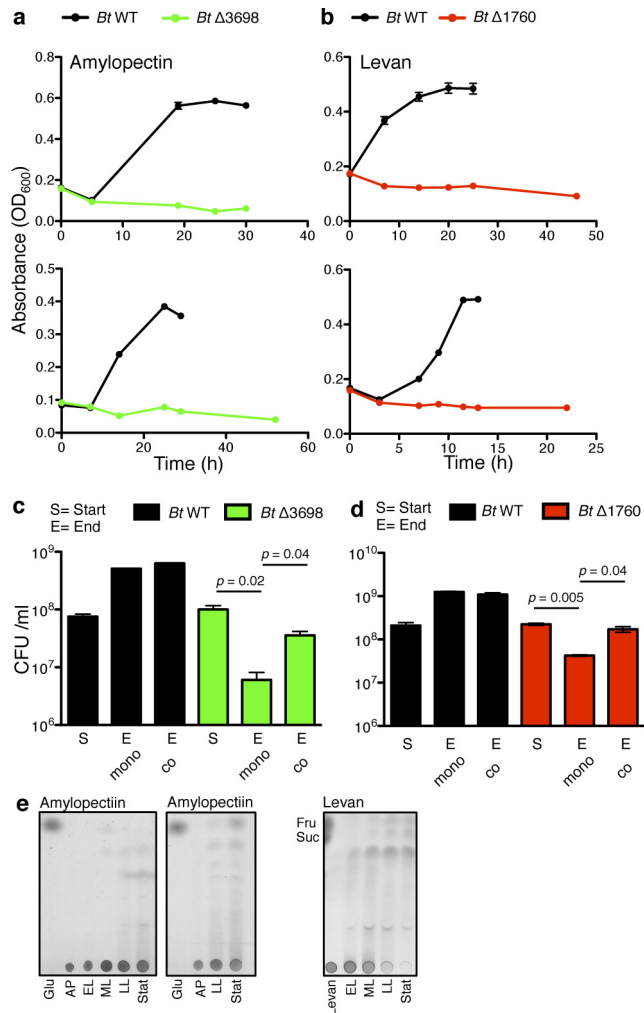
Extended Data Figure 1 | Limited cooperation during polysaccharide utilization by *B. thetaiotaomicron*. **a–d**, Independent experiments for Fig. 1b–e. **a**, **b**, Upper panels $n = 2$ biological replicates, lower panels $n = 1$; **c**, **d**, $n = 2$ biological replicates. **e**, TLC analysis of conditioned media from *B. thetaiotaomicron* grown in amylopectin (left panel) or levan (right panel) minimal media. EL, early log; ML, late log; LL, late log; Stat, stationary phase; Glu, glucose; Fru, fructose; Suc, sucrose. See Supplementary Information Fig. 1 for uncropped scanned images. In all panels, error bars represent standard error; *P* values derived from two-tailed Student's *t*-test.
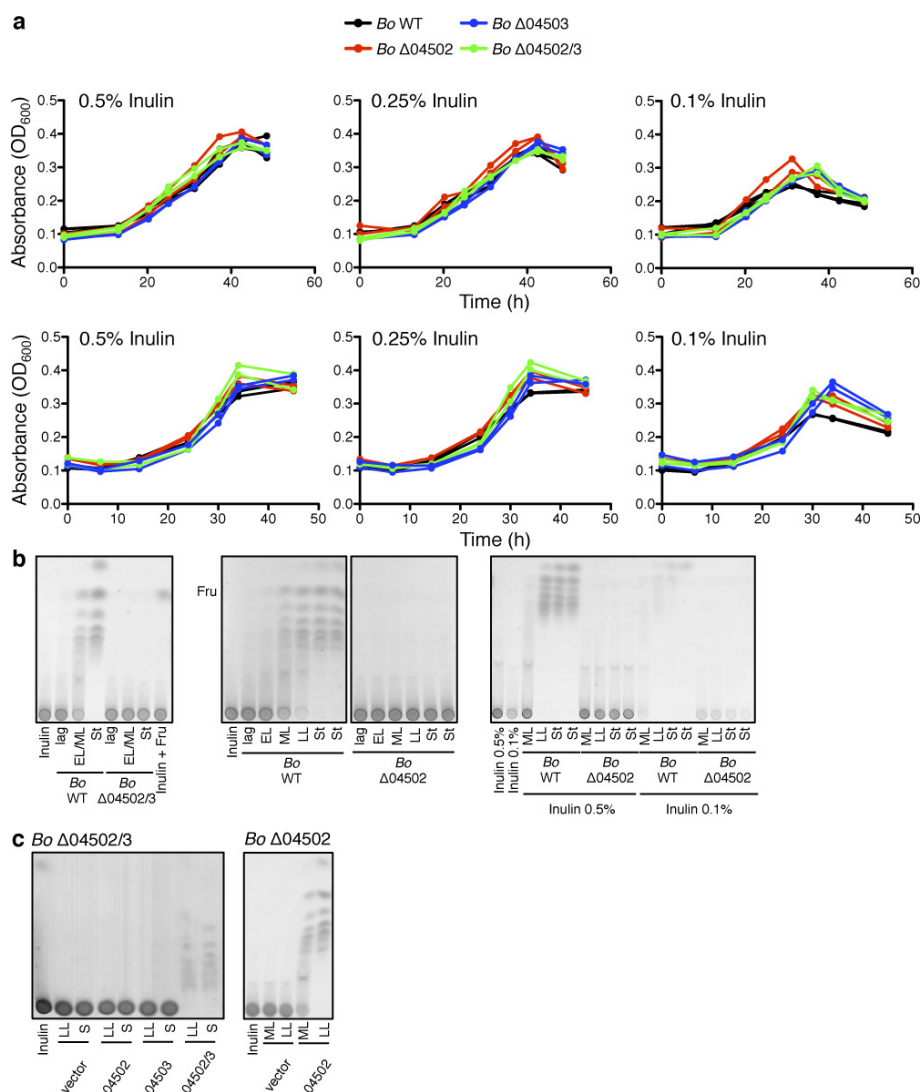
Extended Data Figure 2 | *Bo* 04502 and 04503 mutants grow equivalently to wild type on limiting concentrations of inulin and do not require surface digestion for utilization of inulin. a, Growth of *Bo* WT, Δ04502, Δ04503 and Δ04502/3 mutants in varying concentrations of inulin as indicated. Biological replicates of each condition are plotted as individual lines (*n* = 2 cell culture biological replicates). Upper and lower panels are independent experiments. **b,** Independent experiments for Fig. 2d. EL, early log; ML, mid log; LL, late log; St, stationary phase.

See Supplementary Information Fig. 1 for uncropped scanned images. **c,** Complementation of *Bo* Δ04502 and Δ04502/3 mutants with the respective genes *in trans*. TLC analysis of conditioned media from *Bo* Δ04502/3 (left panel) complemented *in trans* with BACOVA_04502, BACOVA_04503, BACOVA_04502/3 or vector alone (pFD340) and *Bo* Δ04502 (right panel) with BACOVA_04502 or vector alone grown in defined inulin media. See Supplementary Information Fig. 1 for uncropped scanned images. S, stationary phase.

a

b
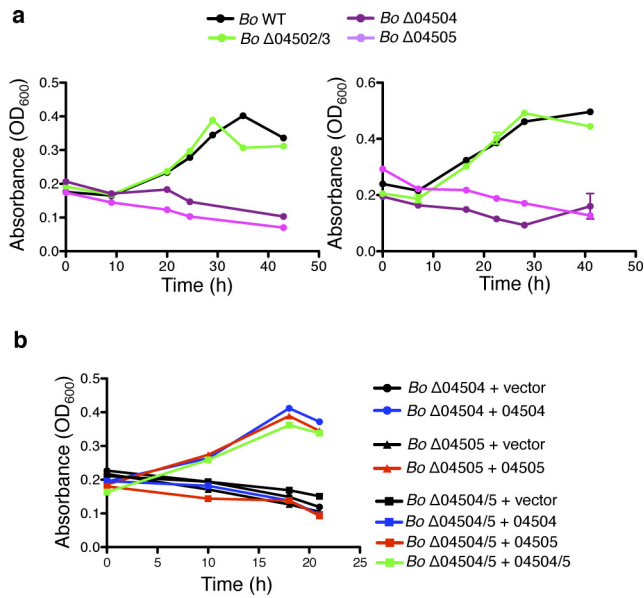
Extended Data Figure 3 | *SusC* and *SusD* homologues BACOVA_04505 and BACOVA_04505 are required for inulin utilization. a, Independent experiments for Fig. 2e. Left panel $n = 2$ biological replicates, right panel each line represents $n = 1$ sample per condition. **b**, Complementation of *Bo* Δ04504, *Bo* Δ04505 and Δ04504/5 mutants with the genes *in trans*. Growth of *Bo* Δ04504, *Bo* Δ04505, *Bo* Δ04504/5 with BACOVA_04504, BACOVA_04505, BACOVA_04504/5 or vector alone (pFD340) *in trans* in defined inulin media. Each line represents $n = 1$ sample per condition. In all panels, error bars represent standard error; P values derived from two-tailed Student's *t*-test.
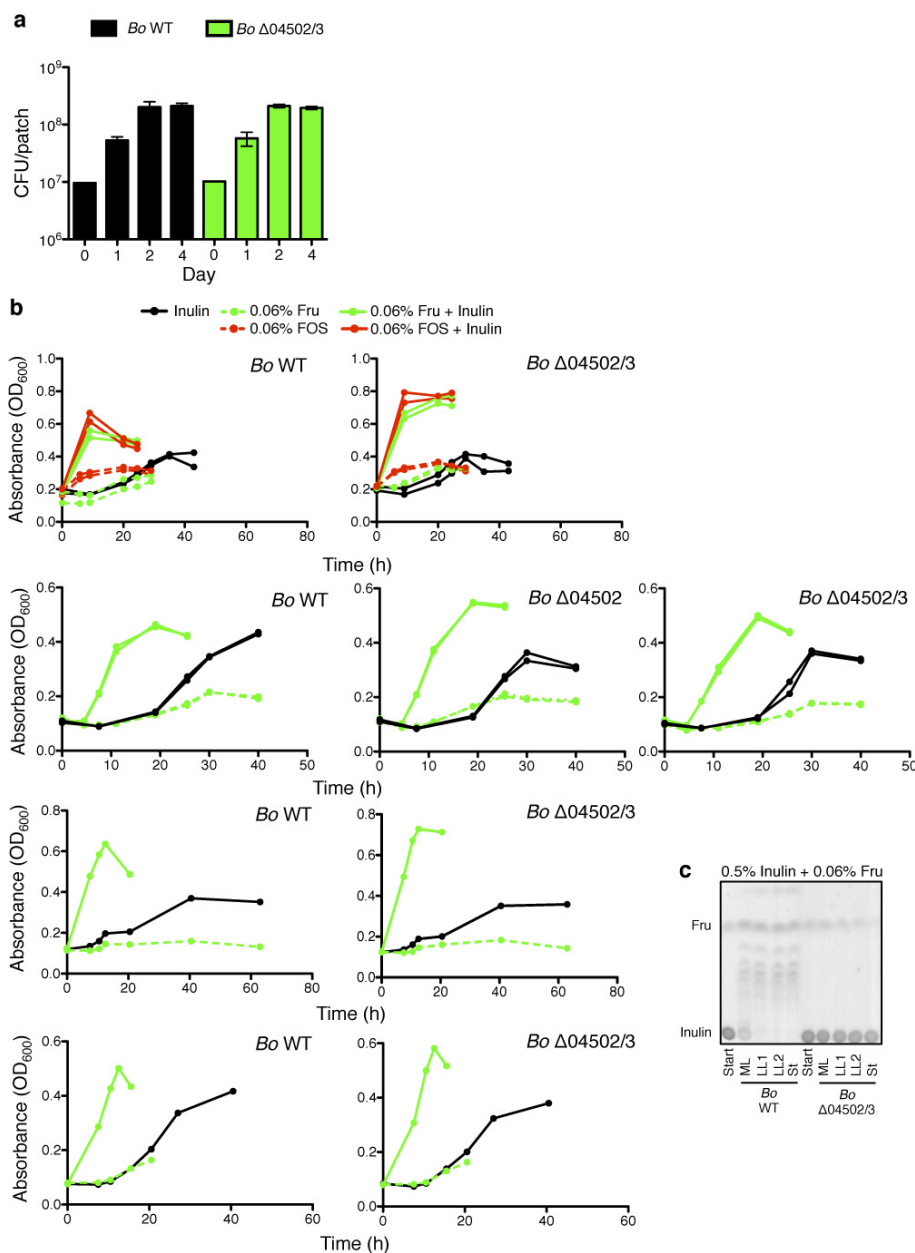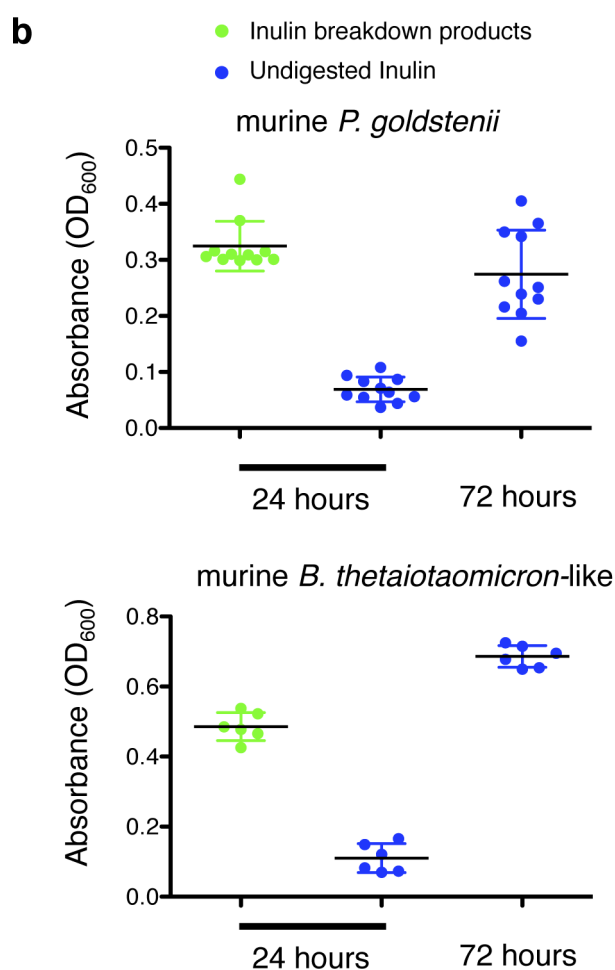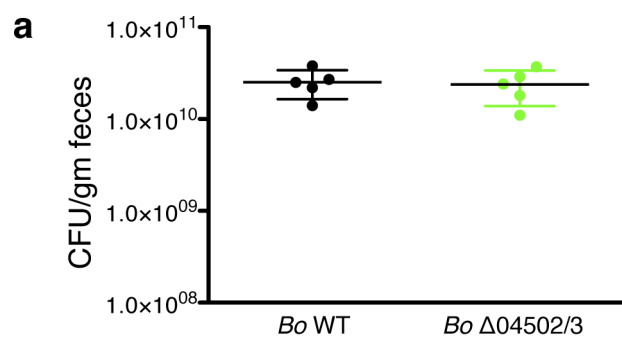
Extended Data Figure 4 | Costs of extracellular inulin digestion by *B. ovatus*. a, **b**, Independent experiments for Fig. 3a, c. $n = 3$ biological replicates at day 1, 2; $n = 2$, biological replicates at day 4 (**a**). In upper and upped middle panels biological replicates of each condition are plotted as individual lines ($n = 2$ cell culture biological replicates); in lower middle and lower panels each line represents $n = 1$ sample per condition (**b**).

c, TLC analysis of conditioned media from *Bo* WT and *Bo* Δ04502/3 cultured in 0.5% inulin with trace (0.06%) amounts of fructose. St, stationary phase. See Supplementary Information Fig. 1 for uncropped scanned images. In all panels, error bars represent standard error; *P* values derived from two-tailed Student's *t*-test.
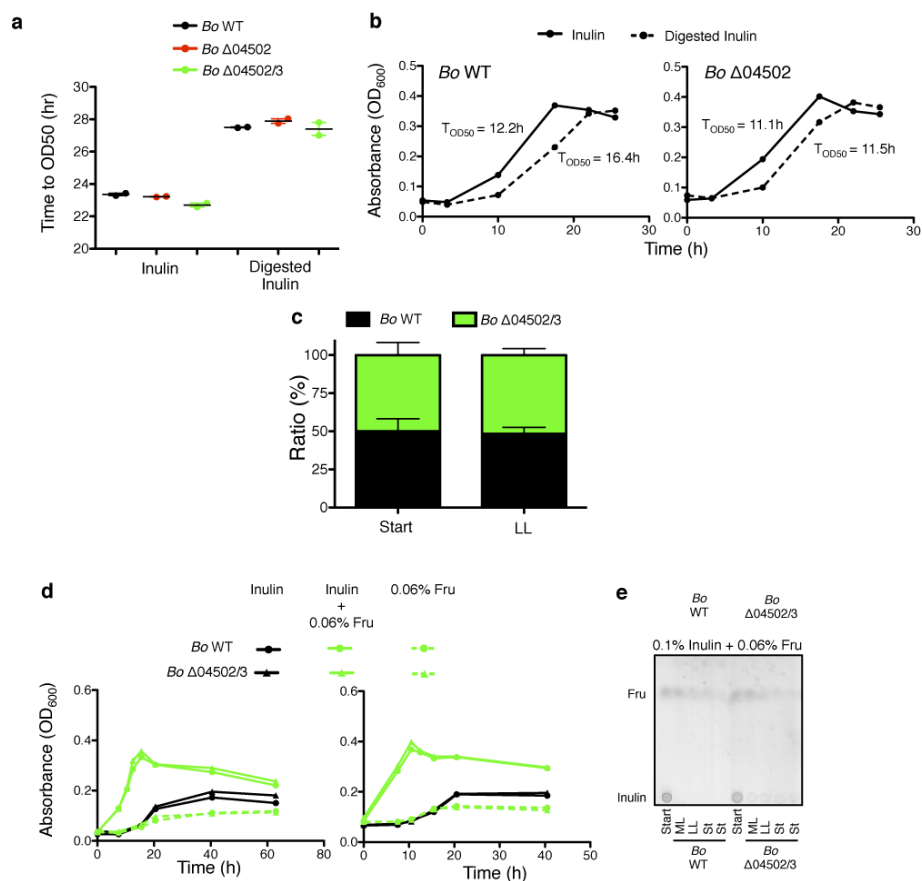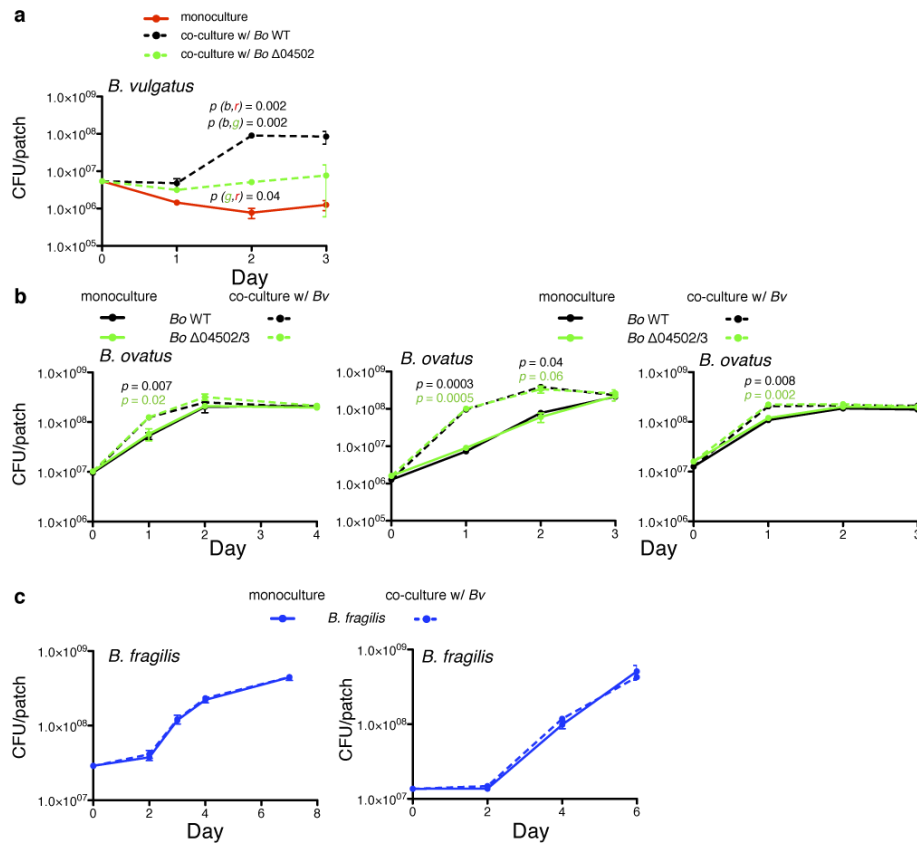
Extended Data Figure 5 | Preferential utilization of undigested inulin by *B. ovatus* and costs of inulin digestion by 04502/3. a, Time to mid-log (estimated at 50% maximal OD (OD50) by linear regression analysis) of Fig. 3d. **b**, Additional independent experiments for Fig. 3d. Each line represents $n = 1$ sample per condition. **c**, Competition of *Bo* WT and *Bo* Δ04502/3 co-cultured in 0.5% inulin with trace (0.06%) amounts of fructose. $n = 2$ cell culture biological replicates; **d, e**, Growth (**d**) and TLC analysis of conditioned media (**e**) of *Bo* WT and *Bo* Δ04502/3 cultured in 0.1% inulin with trace (0.06%) amounts of fructose. See Supplementary Information Fig. 1 for uncropped scanned images. For **d**, each panel is an independent experiment. Each condition is plotted as individual lines in each panel ($n = 2$ cell culture biological replicates). In all panels, error bars represent standard error; *P* values derived from two-tailed Student's *t*-test.

a

b

- Inulin breakdown products
- Undigested Inulin

murine *P. goldstenii*

murine *B. thetaiotaomicron*-like

Extended Data Figure 6 | A complex mouse microbiota differentially affects *B. ovatus* WT and Δ04502/3 pre-colonized gnotobiotic mice and analysis of cross feeding of the predominant murine Bacteroidales of the murine gut microbiota. a, Germ-free mice were monocolonized with *Bo* WT or Δ04502/3 and maintained on a diet supplemented with inulin as the sole polysaccharide and housed under gnotobiotic conditions for 2 weeks. Bacteria were enumerated from faeces before gavage with intestinal microbiota of conventionally raised mice ($n = 5$ mice, cell culture biological replicates). **b**, Growth of two dominant mouse microbiota Bacteroidales strains (*Parabacteroides goldsteinii* and a strain with 96% 16S rRNA gene identity to *B. thetaiotaomicron*) with inulin breakdown products derived from the conditioned media of *B. ovatus* grown in inulin (all inulin had been digested) or undigested inulin minimal media. Each data point is a different isolate of the indicated species from the caeca of the conventionally raised mice used for gavage ($n = 11$ isolates for upper panel, $n = 6$ for lower panel). In all panels, error bars represent standard error.

a

B. vulgatus

- monoculture
- co-culture w/ *Bo* WT
- co-culture w/ *Bo* Δ04502

$p\,(b,r) = 0.002$
$p\,(b,g) = 0.002$
$p\,(g,r) = 0.04$

CFU/patch

b

monoculture   co-culture w/ *Bv*

- *Bo* WT
- *Bo* Δ04502/3

B. ovatus

$p = 0.007$
$p = 0.02$

$p = 0.0003$
$p = 0.0005$

$p = 0.04$
$p = 0.06$

monoculture   co-culture w/ *Bv*

- *Bo* WT
- *Bo* Δ04502/3

B. ovatus

$p = 0.008$
$p = 0.002$

c

monoculture   co-culture w/ *Bv*

- *B. fragilis*

B. fragilis

Extended Data Figure 7 | The *B. ovatus*, but not *B. fragilis* benefits from *B. vulgatus* in co-culture in inulin. a, b, Independent experiments for Fig. 4b, d. The left panel corresponds to starting culture with ∼10^7 CFU *Bo* corresponding to starting culture of ∼10^6 CFU *Bo* in Fig. 4d. The two right panels are a duplicate pair of experiments of starting CFU of 10^6 and 10^7. In each panel $n = 2$ biological replicates. **c,** Enumeration of *B. fragilis* in monoculture or co-culture with *Bv* on defined inulin plates,

$n = 3$ cell culture biological replicates. Letters in parentheses refer to values correlating to colour of line used for statistical analysis. In **a**, for example, $p\,(g,r)$ refers to comparison of values of green (*g*) and red (*r*) values at the time-point indicated. In **b**, colour of *P* value indicates comparison of monoculture and co-culture for the given condition at the time-point indicated. For all panels, error bars represent standard error; *P* values derived from two-tailed Student's *t*-test.
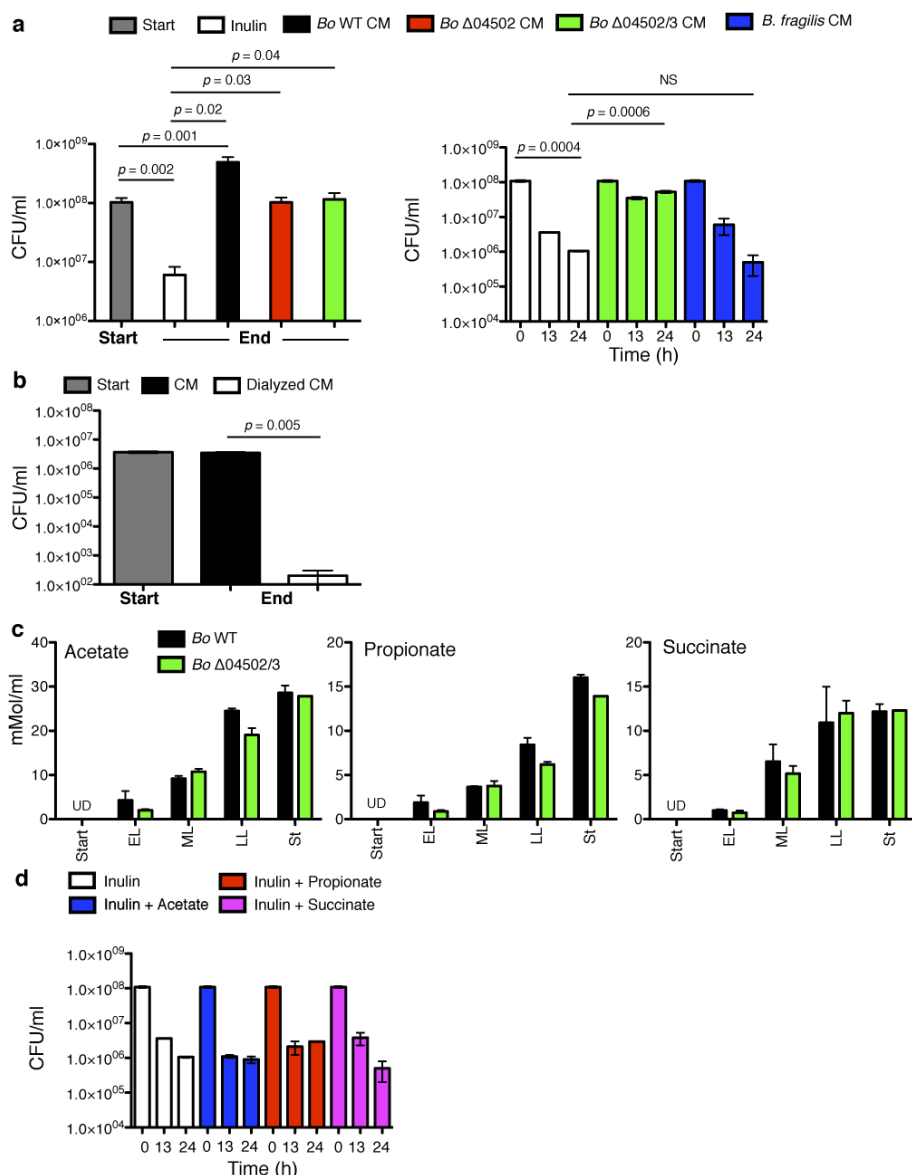
Extended Data Figure 8 | Secreted factors from *Bo* and isogenic mutants, but not *B. fragilis (Bf)*, support *Bv* survival. a, Growth of *Bv* in conditioned media from *Bo* WT, Δ04502, Δ04502/3 or *Bf* grown in defined media with inulin as the sole carbohydrate and in inulin media. End time-point corresponded to peak growth of *Bv* in conditioned media derived from *Bo* WT. *B. fragilis*, which utilizes inulin[1,3] but similar to *Bo* Δ04502/3 does not liberate inulin breakdown products[3], does not support the survival of *Bv* during co-culture. Left and right panels are independent experiments. Left panel; start, $n = 4$ biological replicates; end, $n = 2$ biological replicates. Right panel; t0, $n = 4$ cell culture biological replicates; t13 and 24, $n = 2$ biological replicates. **b**, Growth of *Bv* in dialysed (2 kDa MW membrane) or undialysed conditioned media from

Bo Δ04502/3 grown in inulin, $n = 2$ cell culture biological replicates. **c**, Gas chromatographic analysis of acetate, propionate and succinate in conditioned media during growth of *Bo* WT and Δ04502/3 in defined media with inulin as the sole carbohydrate. Other volatile and non-volatile substances (as listed in Methods) were undetectable, $n = 2$ cell culture biological replicates, except Δ04502/3 stationary phase, $n = 1$. **d**, Growth of *Bv* in defined medium with inulin as the sole carbohydrate with or without addition with 15 mM of acetate, propionate or succinate, $t = 0$, $n = 4$ biological replicates; $t = 13$ and 24 h, $n = 2$ biological replicates. CM, conditioned media; UD, undetected. For all panels, error bars represent standard error; *P* values derived from two-tailed Student's *t*-test.
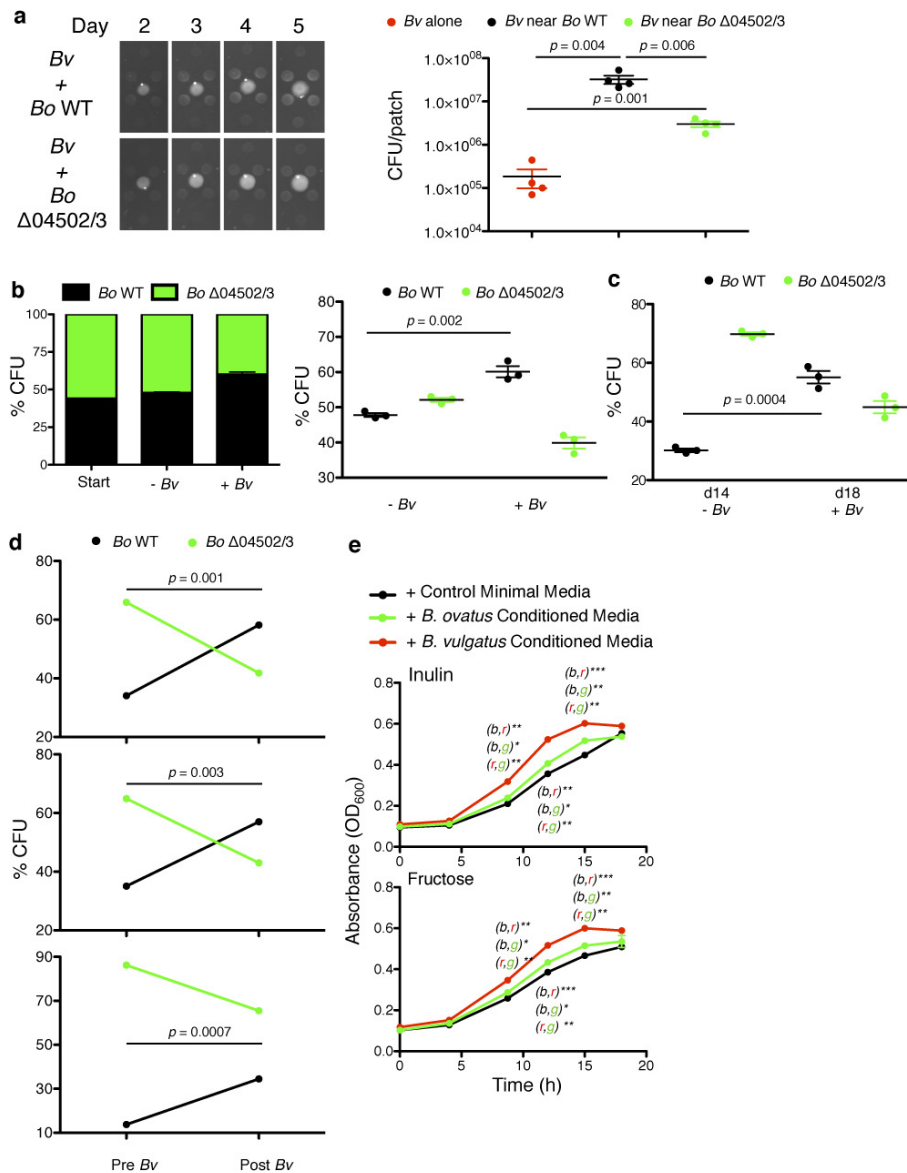
Extended Data Figure 9 | Spatial aspects of mutualism between *Bo* and *Bv* via cross feeding and interspecies cooperation *in vivo* via 04502/3. **a**, Independent experiments for Fig. 4c, $n = 4$ biological replicates. **b**, Independent experiments for Fig. 4e, $n = 3$ cell culture biological replicates. **c**, Scatter plot of experiment in Fig. 4f, $n = 3$ cell culture biological replicates. **d**, Ratios of wild type and Δ04502/3 in faeces 21 days after co-colonization of three germ-free mice ($n = 3$ mice biological replicates) on a diet of inulin as the sole dietary polysaccharide (pre-*Bv*) and then four days after introduction of *Bv* (post-*Bv*). Each panel shows the ratio pre- and post- *Bv* of an individual mouse. *P* values are Fisher exact test comparing the frequency of *Bo* WT and Δ04502/3 pre- and post- colonization with *Bv* for each individual mouse. At day 21, all mice were colonized with a higher ratio of the mutant (ranging to 86%

in the mouse depicted in the lowest panel), with each mouse showing a statistically significant increase in the proportion of the wild type after introduction of *Bv*. **e**, Growth of *B. ovatus* in 0.5% inulin (upper panel) or fructose (lower panel) in minimal media to which filter sterilized conditioned media from early log, $A_{600\,nm}$ matched growth of *Bv* or *Bo* in 0.125% fructose minimal media or fresh 0.125% fructose minimal media control was added at 1:1 ratio. In **e**, numbers refer to *P* values (*$P < 0.05$, **$P < 0.01$, ***$P < 0.001$) of comparison of values of green (*g*), red (*r*) or black (*b*) values by unpaired, two-tailed student *t*-test at the time-point indicated, $n = 2$ cell culture biological replicates. For all panels, error bars represent standard error; for all panels except **d**, *P* values derived from two-tailed Student's *t*-test.
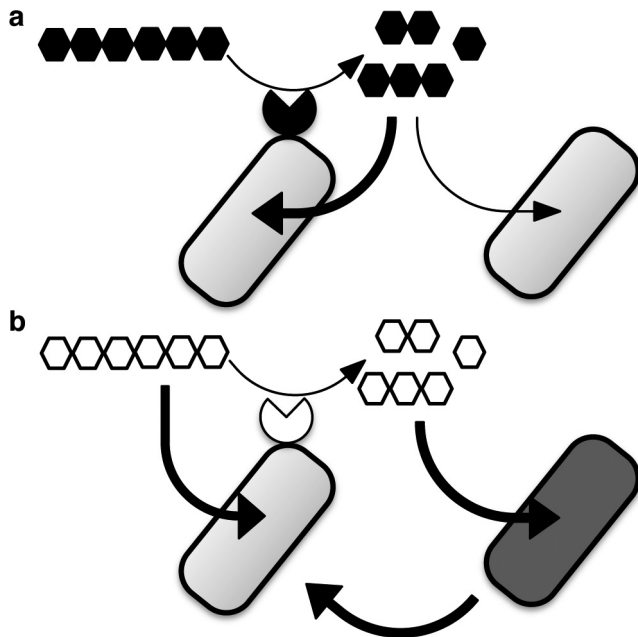
Extended Data Figure 10 | Schematic of forms of cooperativity via polysaccharide digestion among Bacteroidales. a, Limited cooperation. Privatization of extracellularly digested public goods by the individual performing the digestion leads to greater individual (thick arrow) than shared benefits (thin arrow) as seen in *Bt* during growth on levan and amylopectin. **b**, Cooperation between species is seen between *Bo* and *Bv* during growth on inulin. Surface digestion of inulin by *Bo* creates breakdown products that it does not need to grow on inulin. Rather, inulin breakdown represents a dedicated cross-feeding system that provides benefits to *Bv*, with reciprocal fitness benefits to *Bo*.